

PAPER • OPEN ACCESS

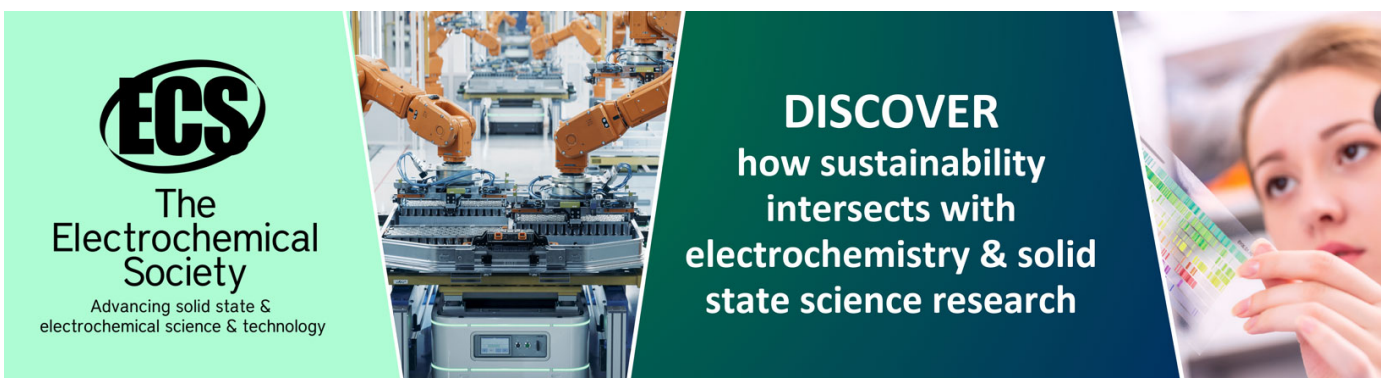
High Temperature Thermal Properties of Columnar Ytria Stabilized Zirconia Thermal Barrier Coating Performed by Suspension Plasma Spraying

To cite this article: B Bernard *et al* 2016 *J. Phys.: Conf. Ser.* **745** 032012

View the [article online](#) for updates and enhancements.

You may also like

- [A comparative study on the microstructure, hot corrosion behavior and mechanical properties of duplex and functionally graded nanostructured/conventional YSZ thermal barrier coatings](#)
T Samani, M Kermani, M Razavi et al.
- [A real time deformation evaluation method for surface and interface of thermal barrier coatings during 1100 °C thermal shock](#)
Xiaobo Yang, Zhanwei Liu and Huimin Xie
- [Columnar-structured thermal barrier coatings deposited via the water-based suspension plasma spray process](#)
Pengyun Xu, Guohui Meng, Guijie Liu et al.



ECS
The
Electrochemical
Society
Advancing solid state &
electrochemical science & technology

DISCOVER
how sustainability
intersects with
electrochemistry & solid
state science research

High Temperature Thermal Properties of Columnar Yttria Stabilized Zirconia Thermal Barrier Coating Performed by Suspension Plasma Spraying

B Bernard^{1,2}, V Schick², B Remy², A Quet¹, L Bianchi³

¹CEA-DAM, Le Ripault, BP16, 37260, Monts, France

²LEMETA, Université de Lorraine, 2 Avenue de la forêt de Haye, TSA 60604, 54518, Vandoeuvre-lès-Nancy cedex, France

³Safran, Pôle Matériaux et procédés, rue des Jeunes Bois, Châteaufort, CS 80112, 78772, Magny-les-Hameaux, France

www.benjamin.bernard@cea.fr

Abstract. Performance enhancement of gas turbines is a main issue for the aircraft industry. Over many years, a large part of the effort has been focused on the development of more insulating Thermal Barrier Coatings (TBCs). In this study, Yttria Stabilized Zirconia (YSZ) columnar structures are processed by Suspension Plasma Spraying (SPS). These structures have already demonstrated abilities to get improved thermal lifetime, similarly to standard YSZ TBCs performed by EB-PVD. Thermal diffusivity measurements coupled with differential scanning calorimetry analysis are performed from room temperature up to 1100 °C, first, on HastelloyX substrates and then, on bilayers including a SPS YSZ coating. Results show an effective thermal conductivity for YSZ performed by SPS lower than 1 W.m⁻¹K⁻¹ whereas EB-PVD YSZ coatings exhibit a value of 1.5 W.m⁻¹K⁻¹.

1. Introduction

Thermal barrier coatings (TBCs) are widely used in order to prevent thermal degradation and oxidation of metal components of gas turbines such as blades or guide vanes. Over the past decade, one of the main purposes for gas turbine enhancement has been to increase operating temperatures with more insulating TBCs [1].

Until now, TBCs are mainly composed of Yttria Stabilized Zirconia (YSZ). YSZ layers are commonly carried out using the Electron Beam Physical Vapor Deposition process (EB-PVD) that leads to a columnar microstructure [2]. The coefficient of thermal expansion (CTE) mismatch between YSZ and metal substrates involves thermally induced stresses. However, the stress accommodation behavior of columns offers high thermal compliance and induces high lifetime for such TBCs. The main shortcoming is columnar microstructure comes with heat conduction paths that lead to relatively high values of thermal conductivity, around 1.5 W.m⁻¹.K⁻¹ [1].



Recent studies have shown that Suspension Plasma Spraying (SPS) provides microstructures including multi-scaled porosity [3]. Small particles (from a few nanometers to 5 μm) are injected through a plasma jet using a liquid carrier medium (water, ethanol,...) to be accelerated and melted in order to spread them over a metal substrate [4]. This technique is the result of the development of Atmospheric Plasma Spraying (APS) where particles $> 5 \mu\text{m}$ are commonly injected using a carrier gas. Decreasing the size of injected particles for SPS compared to the APS process allows to reach new coating build-up and new microstructures far from the typical lamellar one of APS. Particularly, SPS allows to reach columnar microstructures [5,6]. This specific microstructure is directly linked to the reduction in size of sprayed materials [5] and has been identified as promising for TBC enhancement showing some improved properties in terms of thermal lifetime [6].

The aim of this work is to investigate thermal properties of SPS columnar structures from room temperature up to 1100°C. Process parameters are optimized to obtain a high uniformity in size of columns in the top surface of the coatings, as described in a previous study [7]. The effective thermal conductivity is determined using thermal diffusivity and specific heat capacity experimental measurements for both substrate and the SPS coating. A bilayer model including heat losses is used to estimate thermal diffusivity from flash experiments. Differential scanning calorimetry (DSC) allows the measurement of the specific heat capacity.

2. Coating production and microstructure analysis

YSZ ethanol-based suspensions, with 7 wt % Y_2O_3 and medium particle diameters lower than 300 nm, are purchased from Treibacher Industrie AG. Coatings are carried out onto Hastelloy X substrates with an aluminized NiAl bond coat. In order to improve adhesion of the YSZ layer, a thin Thermally Grown Oxide (TGO) layer of Al_2O_3 is obtained by the bond coat oxidation with a heat treatment at 1100°C for 1 h.

A F4-VB type plasma torch with a 6 mm internal diameter nozzle (Oerlikon-MetcoTM, Wohlen, Switzerland) is used to perform YSZ coatings. Coatings are achieved into a ventilated booth maintained at atmospheric pressure and substrate cooling is ensured by compressed air and liquid CO_2 spraying. Suspension is stored and stirred into a pressurized vessel and injected radially through a nozzle into the plasma jet. An illustration of the SPS process is given in Figure 1. Spraying conditions, described in Table 1, leading to an optimized columnar structure as described elsewhere [7].

Table 1. Spraying parameters

	Spraying condition
Plasma gas mixture	Ar/He/ H_2
Plasma enthalpy (kJ/g)	2.2×10^7
Power (kW)	32.2
Plasma mass gas rate (g/s)	1.5
Standoff distance (mm)	50
Suspension feed rate (g/min)	25
Torch linear speed (m/s)	1.5

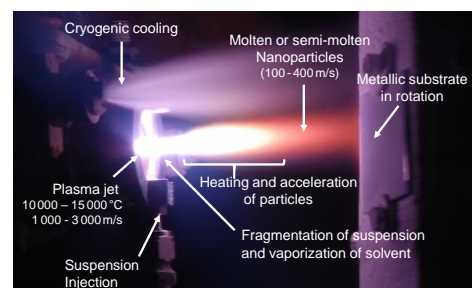


Figure 1. Illustration of the SPS process during deposition of YSZ on a metallic substrate

Microstructures are observed using Scanning Electron Microscopy (SEM) on a Leo 435VPi microscope. The coating density, ρ_c , is estimated by image analysis of SEM cross-section using ImageJ software. SEM images are converted into binary images for porosity measurement. Then the value of ρ_c is calculated using equation (1) where P is the porosity and ρ_{YSZ} the theoretical value of YSZ bulk density taken as 6053 $\text{kg}\cdot\text{m}^{-3}$ from literature [8]. Error on porosity is estimated at 5 % of the measurement.

$$\rho_c = \rho_{YSZ}(1 - P) \quad (1)$$

3. Characterization methods of thermal properties

3.1. Thermal diffusivity

3.1.1. Methodology and devices. High temperature thermal diffusivity measurements are achieved on a high temperature experimental bench developed at LEMTA. Samples are placed into a temperature controlled tubular furnace heating from room temperature up to 1100 °C under air. Flash is performed using an impulse 300 μs Quantel laser allowing to deliver an energy of 50 J at the wavelength of 1053 nm. The impulse presents a Gaussian temporal shape allowing to consider for the model described in the present study the excitation source as a Dirac response for the flow. The evolution of the rear face temperature is recorded using a highly sensitive cooled matrix infrared InSb detector [1.5 – 5.5 μm] Cedip® Titanium SC7000. YSZ, and moreover plasma sprayed YSZ, presents a semi-transparency behaviour for the detection wavelength [9,10,11]. In order to overcome the semi-transparency of YSZ in infrared wavelength, a thin layer of graphite (around 10-20 μm) is applied to the surface of SPS coatings. Thus, heat transfers considered totally neglected radiation contribution leading to the effective thermal conductivity estimation. As the SPS YSZ layer is coated on a metallic substrate, heat equation needs to be solved considering the sample as bilayer in order to perform a numerical estimation of the thermal properties of the SPS layer. Two measurements are necessary to achieve the thermal diffusivity measurement of the YSZ coating. First, the substrate is characterized uncoated in order to estimate the value of its thermal diffusivity. Then, a second measurement of the bilayer sample (substrate and YSZ) is performed to estimate the SPS coating thermal diffusivity knowing the thermal properties of the substrate material.

3.1.2. Model. The numerical reconstruction of thermograms is done by solving the heat equation in Laplace's space using thermal quadrupole method as described by Maillet *et al.* [12]. The heat equation can be written in Laplace's space using equation (2)

$$\Phi(z, p) = -\lambda S \frac{d\Theta(z, p)}{dz} \quad \text{and} \quad \lambda = \alpha \rho Cp \quad (2)$$

In equation (2), S represents the illuminated surface, λ the thermal conductivity, α is the thermal diffusivity, ρ , the layer density, Cp , the heat capacity and $\Phi(z, p)$ and $\Theta(z, p)$ are the Laplace transforms of the heat flow φ and the temperature T , respectively. The two Laplace transforms can be expressed by the following equations (3) and (4), where t represents the time and p the Laplace variable.

$$\Theta(z, p) = \int_0^{\infty} T(z, t) \exp(-pt) dt \quad (3) \quad \text{and} \quad \Phi(z, p) = \int_0^{\infty} \varphi(z, t) \exp(-pt) dt \quad (4)$$

By considering heat losses h , which are the same on both sides of the sample of thickness e ($h = h_{z=0} = h_{z=e}$), and a unique source of energy at $z = 0$ typed q_0 , equation (1) can be solved using the two following limit conditions (equations (5) and (6)).

$$\varphi_{z=0} = \left. \frac{\partial T}{\partial z} \right|_{z=0} = q_0 - hS(T_0 - T_{\infty}) \quad (5) \quad \text{and} \quad \varphi_{z=e} = \left. \frac{\partial T}{\partial z} \right|_{z=e} = hS(T_e - T_{\infty}) \quad (6)$$

The solution is given using the quadrupole formalism in the Figure 2. Subscripts s and c correspond to the responses of the substrate and the coating, respectively. The expression of the Laplace temperature on the rear face $\Theta_c(z, p)$ is expressed in equation (7)

$$\Theta_e(z, p) = \frac{1}{A+Bh+Ch^2} \tag{7}$$

Where: $A = C_s A_d + A_s C_d$; $B = 2A_s A_d + B_s C_d + C_s B_d$; $C = A_s B_d + B_s A_d$

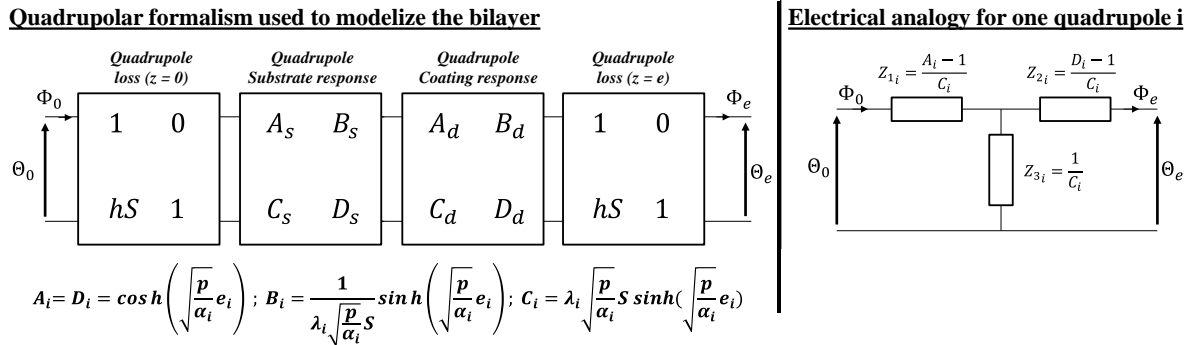


Figure 2. Equivalent electric representation obtained by quadrupole method. It describes the experimental setup in the Laplace's space.

By using De Hoog algorithm [13], a numerical inversion is performed in order to reconstruct thermograms in time. Values of α , ρC_p and λ are then adjusted in order to fit the most exactly possible to the experimental curve using least square method [14,15]. Sensitivities of the fitting parameters to numerical inversion is calculated using the contrast method [16]. This method is illustrated by Figure 4 (a) where the contrast curve is obtained by deducting the bilayer response to the uncoated substrate response. Sensibilities to parameter K_1 (thermal diffusivity ratio) and K_3 (heat capacity ratio) is then calculated, and can expressed by following equations (8). As shown in Figure 4 (b), only K_1 is sensible to the De Hoog inversion allowing to only make an accurate estimation of the thermal diffusivity of the coating. For this reason, K_3 is fixed during estimation in order to ensure a good accuracy of the estimation of thermal diffusivity of the coating. Heat capacity is obtained using differential scanning calorimetry (DSC) and the coating density by image analysis.

$$K_1 = \frac{e_c}{e_s} \sqrt{\frac{\alpha_s}{\alpha_c}} \quad \text{and} \quad K_3 = \frac{e_c \rho_c C_{p_c}}{e_s \rho_s C_{p_s}} \tag{8}$$

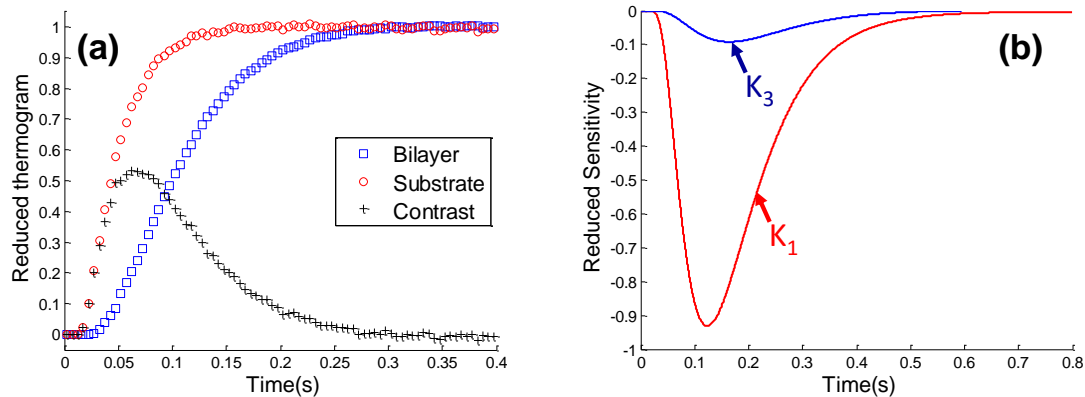


Figure 4. Contrast curve between uncoated substrate and the bilayer sample (a) and sensitivities to contrast coefficient K_1 and K_3 (b)

3.2. Specific heat capacity

Differential scanning calorimetry (DSC) is used for measurement of specific heat capacity C_p of the substrate and the SPS coating. A Setaram Micro Sc3 is used to performed DSC analysis at room temperature. A Setaram 96 Line_{ev0} DSC device is used to performed high temperature measurements from 200°C up to 1100 °C. The powder obtained from a delaminated YSZ coating is used for the estimation of the heat capacity of coating. Errors represent 5 % of the measurements.

4. Results and discussion

4.1. Description of microstructure

A typical SPS columnar structure is produced similar to those observed elsewhere [5,6]. It is characterized by columns separated by inter-columnar voids as shown in Figure 5. Columnar features developing a typical cauliflower shape can be noticed on the top surface. This specific microstructure is assumed to be linked to the used nanosized of the particles. As described by Van Every *et al.* [5], smallest particles could follow the plasma jet and reach a lateral velocity close to the substrate. Indeed, the reduced standoff distance required in SPS enhances the plasma flow deviation close to the substrate resulting in a high deviation of the nanosized particles in the vicinity of the substrate. It leads to a normal and lateral expansion of SPS coatings onto the substrate asperities. The obtained columnar structure presents a high void content of 25 % (intra and intercolumnar), leading to a coating density of 4514 kg.m⁻³.

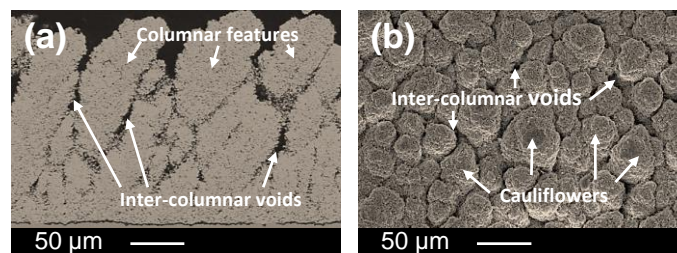


Figure 5. SEM pictures of SPS coating on cross section (a) and top view (b).

4.2. Thermal properties

Measured specific heat capacities of HX substrate and YSZ SPS coating are plotted in Figure 6. Results are compared to literature values [8,17]. It appears that a good reliability is obtained for both materials. The experimental values of the present study, for which errors are estimated around 5 % of the measured value, can be used for the estimation of the thermal diffusivity. In order to ensure a good accuracy for the thermal diffusivity during the numerical reconstruction, C_p and ρ provided by DSC and image analysis, are kept constant and are not used as variable parameters. Mainly the thermal diffusivity and heat losses are considered in the least square estimation.

Thermal diffusivity estimation and thermal conductivity calculation of HX substrate are given in Figure 7 (a) and (b) respectively. Experimental values from the estimation of thermal diffusivities are consistent with reported studies [18]. The addition of the NiAl aluminized bond coat and the formation of a thin Al₂O₃ film do not strongly affect thermal properties compared to the pure Hastelloy X substrate. In fact, the layer of NiAl (around 30-50 μm) represent a negligible thickness compared to the global thickness of the substrate (1.2 mm) and not contribute to thermal properties. Thermal conductivity evolves almost linearly from 10.9 W.m⁻¹K⁻¹ at room temperature to 37 W.m⁻¹K⁻¹ at 1100 °C as shown on Figure 7 (b). Experimental values are then used to estimate the thermal diffusivity and the conductivity of the SPS YSZ coating in the bilayer system.

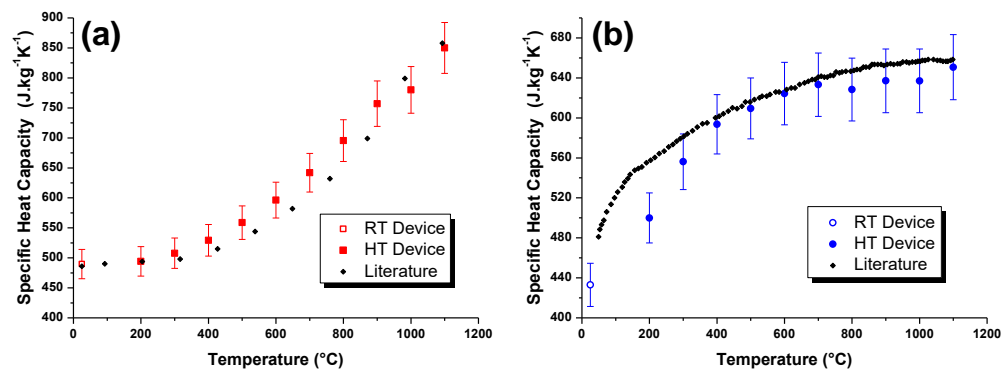


Figure 6. Evolution of heat capacity using room temperature (RT) and high temperature (HT) devices for HX (a) and SPS coating (b). Data extracted from [8,17]

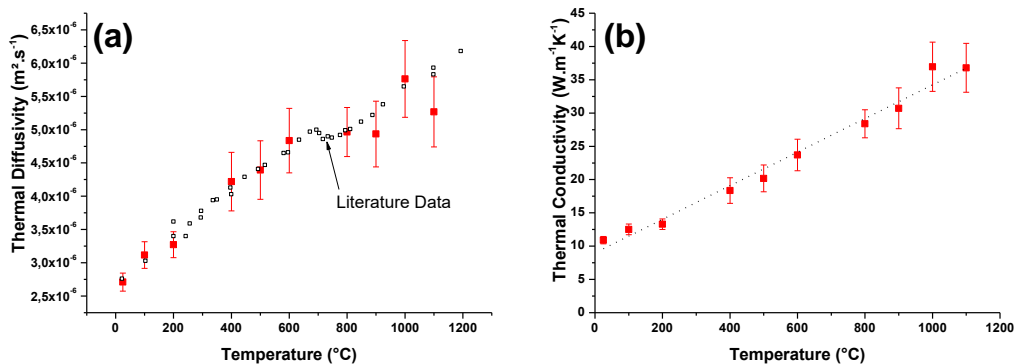


Figure 7. Temperature dependency of thermal diffusivity (a) and thermal conductivity (b) for HX (a). Literature data for HX diffusivity is extracted from [18]

Figure 8 shows experimental thermograms of the HX/YSZ SPS bilayer sample, recorded using the high temperature bench developed at LEMTA, and their numerical reconstruction using the model described in the last section. Estimations of thermograms are performed for a thermal response of 600 ms at each temperature allowing comparisons. The flat profile of residues between experimental values and numerical reconstructions, obtained for all the estimations, allows to appreciate the quality of the thermal diffusivity estimation and ensures a good reliability of values. Examples are given on Figure 8 at 25 $^{\circ}\text{C}$, 500 $^{\circ}\text{C}$, 700 $^{\circ}\text{C}$, 900 $^{\circ}\text{C}$, 1000 $^{\circ}\text{C}$ and 1100 $^{\circ}\text{C}$. It is observed that an increase of temperature increase contribution of heat losses. Thermograms at 900 $^{\circ}\text{C}$; 1000 $^{\circ}\text{C}$ and 1100 $^{\circ}\text{C}$ presented on Figure 8 illustrated the purpose by the rapid decrease of the signal after reach the maximum of intensity close to 300 ms. Results are consistent with the consideration of heat losses for the model.

Estimated thermal diffusivity and resultant thermal conductivity are presented in Figure 9 (a) and (b) respectively. A relative decrease of thermal diffusivity with respect to temperature is observed in Figure 9 (a) which in fact compensate the increase of C_p values for YSZ SPS coating as presented in Figure 6 (b). It leads to a quite flat response in temperature for the thermal conductivity of the ceramic coating with values calculated between $0.7 \pm 0.1 \text{ W.m}^{-1}\text{K}^{-1}$ and $0.9 \pm 0.1 \text{ W.m}^{-1}\text{K}^{-1}$. These thermal conductivities are in the same range of reported values ($0.7 - 1.2 \text{ W.m}^{-1}\text{K}^{-1}$) for similar structures obtained by suspension plasma spraying with an axial injection of suspensions [6].

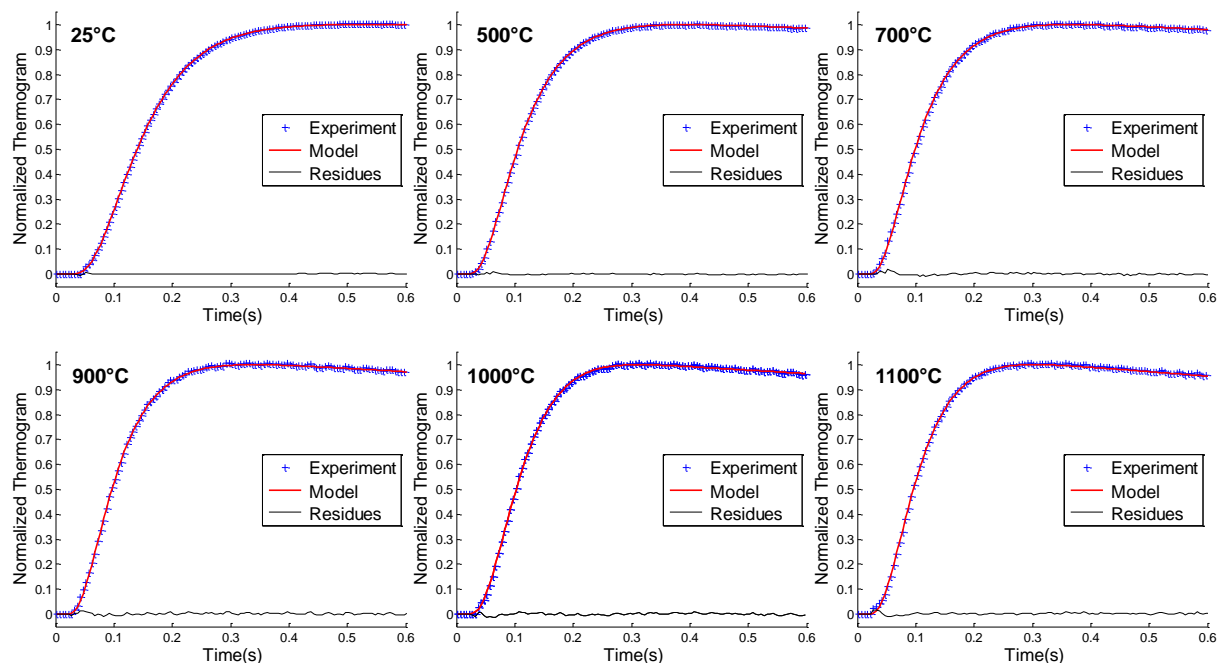


Figure 8. Numerical reconstruction of thermograms of HX/YSZ bilayer at different temperatures.

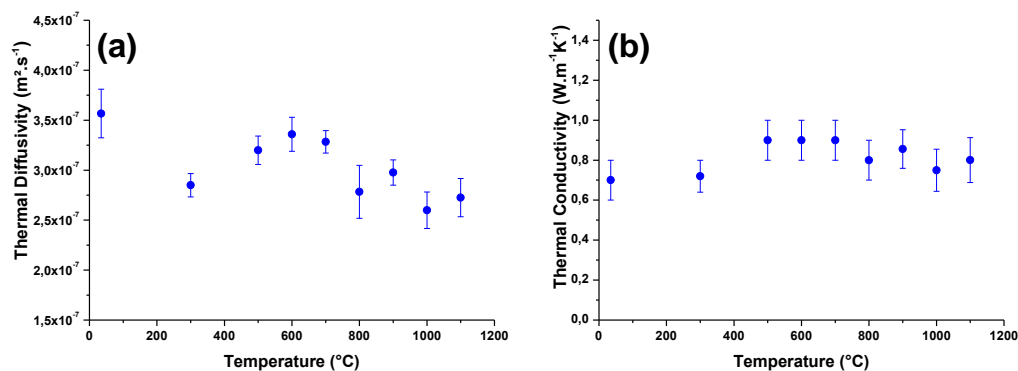


Figure 9. Temperature dependency of thermal diffusivity (a) and thermal conductivity (b) for the SPS coating.

In fact, the high content of small pores of SPS coatings is expected to increase phonon scattering, leading to a low thermal conductivity. These results, showing a thermal conductivity of SPS coatings lower than $1 \text{ W.m}^{-1}\text{K}^{-1}$ at $1100 \text{ }^\circ\text{C}$, are promising for thermal barrier coating enhancement when compared to YSZ coatings performed by EB-PVD ($1.4\text{-}1.5$ at $1100 \text{ }^\circ\text{C}$) [1].

Conclusion

Thermal properties of columnar YSZ coatings produced by suspension plasma spraying are acquired from room temperature up to $1100 \text{ }^\circ\text{C}$. Differential scanning calorimetry and flash laser techniques are employed respectively, to determine specific heat capacity and thermal diffusivity of NiAl aluminized Hastelloy X substrate and YSZ coatings. A bilayer model based on Laplace transforms and quadrupole formalism including heat losses is used to estimate thermal diffusivity. Residues between experimental thermogram and numerical reconstruction ensure reliability of thermal diffusivity values. The thermal conductivity of YSZ coating is found to be lower than $1 \text{ W.m}^{-1}\text{K}^{-1}$ from room temperature up to $1100 \text{ }^\circ\text{C}$. This kind of structure seems to be able to meet the requirements of next generations of gas turbine engines.

The anisotropic SPS columnar structure is also particularly interesting for further thermal diffusivity measurements. Using a coupled Laplace and Fourier-cosine transform approach to solve the heat equation through the bilayer, the estimation of the in-plane thermal diffusivity, as well as the thermal diffusivity in the thickness of the sample, can be achieved using one measurement as described elsewhere for a monolayer material [19]. This kind of transforms is illustrated by the following equation (8). The use of these transforms induces a system of equations only depending on space variables that can also be solved using a quadrupole approach [12].

$$\theta(\alpha_n, \beta_m, z, t) = \int_{t=0}^{+\infty} \int_{x=0}^{x=L} \int_{y=0}^{y=L} (T(x, y, z, t) - T_{\infty}) \cos(\alpha_n x) \cos(\beta_m y) \exp(-pt) dx dy \quad (8)$$

Even if YSZ semi transparency is supposed to be overcome using a carbon layer, the implementation of radiative consideration could greatly enhance the thermal conductivity characterization of these kind of TBCs. Indeed, transport scattering coefficient is strongly influenced by the pore radius and could be treated as an effect of polydisperse spherical pores in the ceramics [20]. Datas from USAXS measurements could be useful for take into account the multi-scaled porosity observed in SPS coatings in a model including radiation considerations [3].

References

- [1] Schultz U, Saruhan B, Fritscher K and Leyens C 2004 *Int. J. Appl. Ceram. Technol.* **1** 302
- [2] Schulz U, Menzebach M, Leyens C and Yang Y 2011 *Surf. & Coat. Technol.* **146-147** 117
- [3] Bacciochini A, Ilavsky J, Montavon G, Denoirjean A, Ben-Ettouil F, Valette S, Fauchais P and Wittmann-Teneze K 2010 *Mat. Sci. and Eng. A* **528** 91
- [4] Pawlowski L 2009 *Surf. & Coat. Technol.* **203** 2807
- [5] Van Every K, Krane M, Trice W, Wang H, Porter W, Besser M, Soderlet D, Ilavsky J and Almer J 2011 *J. Therm. Spray. Technol.* **20** 817
- [6] Curry N, Van Every K, Snyder T and Markocsan N 2014 *Coatings* **4** 630
- [7] Bernard B, Bianchi L, Malié A, Joulia A and Rémy B 2016 *J. Europ. Ceram. Soc.* **36** 1081
- [8] Mévrel R, Laizet J, Azzopardi A, Leclercq B, Poulain M, Lavigne O and Demange D 2004 *J. Europ. Ceram. Soc.* **24** 3081
- [9] Eldridge J and Spuckler C 2008 *J. Am. Ceram. Soc.* **91** 1603
- [10] Eldridge J, Spuckler C and Markham R 2009 *J. Am. Ceram. Soc.* **92** 2276
- [11] Dombrovsky L, Rousseau B, Echegut P, Randrianalisoa J and Baillis D 2011 *J. Am. Ceram. Soc.* **94** 4310
- [12] Maillet D, André S, Batsale J, Degiovanni A and Moyne C 2000 *Thermal Quadripoles Solving the Heat Equation through Integral Transforms* (Wiley).
- [13] De Hoog F, Knight JH and Stokes AN 1982 *S.I.A.M. J. Sci. and Stat. Comp.* **3** 357
- [14] Levenberg K 1944 *Quart. Appl. Math.* **2** 164
- [15] Marquardt D 1963 *J. Soc. Ind. Appl. Mathem.* **11** 68
- [16] Rémy B, André S and Maillet D 2011 *Non linear parameter estimation problems: tools for enhancing metrological objectives* (France: Eurotherm Metti 5 Spring School) lecture 4 .
- [17] <http://www.haynesintl.com/HASTELLOYXAlloy/HastelloyXAlloyPP.htm> the 13 January 2016
- [18] Mills K 2002 *Recommended values of Thermophysical properties for selected commercial Alloy*, (England: Woodhead publishing Ltd and ASM) p177
- [19] Souhar Y, Rémy B and Degiovanni A. 2013 *Int J Thermophys* **34** 322
- [20] Dombrovsky L, Tagne H, Baillis D and Gremillard L 2007 *Infrared Phys. Tech.* **51** 44

Acknowledgments

Authors thank André Malié from Safran-Snecma for providing Hastelloy X with aluminized NiAl coating as substrates and Aurélien Joulia from Safran group for helpful discussions.